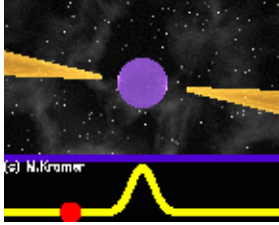

Pulsar Studies with the Shanghai TianMa Radio Telescope

Speaker： Zhen Yan*

Shanghai Astronomical Observatory, CAS

*On behalf of the Shanghai TianMa Radio Telescope Team

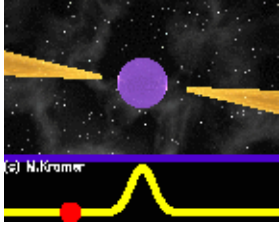

Outline

- Introduction to Shanghai TianMa Radio Telescope
  - The history of TRMT
  - Receivers of TMRT
  - The pulsar backend of TMRT
- Some pulsar observation results
  - Magnetar in the Galactic center
  - Multi-frequency observation
  - Pulsar timing
  - Pulsar hunting
  - Pulsar astrometry with VLBA+TMRT
- Conclusion

troduction to Shanghai TianMa radio telesco

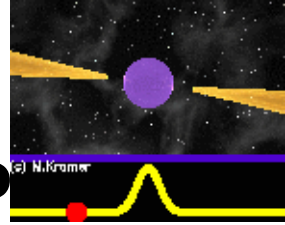

- Newly built 65-m in diameter fully steerable radio telescope located in Song-Jiang district of Shanghai city;
- It is called Tianma Radio Telescope (TMRT),because it is near the small mountain named TianMa;

- Phase of the SH-65m project
  - Funded in 2008;
  - Started manufacturing in 2009;
  - 1st phase was finished in July 2013, four low frequency receivers (L,S,C,X) have been installed.
  - Have been expanded to Q-band (43GHz) in 2017 using active surface system to make sure its efficiency

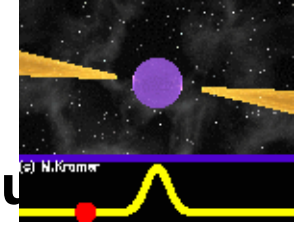

Comparison TMRT with others of the same architectu

Frequency: 1.25-50.0 GHz, eight receivers; four low frequency receivers which are suitable for normal pulsar observations.

		GBT	Effelsberg	Parkes	Lovell	Tianma
L	Freq-R	1.15-1.73	1.27-1.45, 1.59-1.73	1.2-1.8	1.25-1.50, 1.55-1.73	1.25-1.75
	SEFD	10	20,19	31	36,65	31
S	Freq-R	1.73-2.6	2.20-2.30	2.2-2.5	-----	2.2-2.4
	SEFD	12	300	25	-----	≥31
C	Freq-R	3.95-5.85	5.75-6.75	4.5-5.1	6.0-7.0	4.0-8.0
	SEFD	10	25	61	80	28
X	Freq-R	8.00-10.1	7.9-9.0	8,1-8.7	-----	8.2-9.0
	SEFD	15	18	170	-----	≥38

Note: **System Equivalent Flux Density** (SEFD): $SEFD = \frac{2k_B T_{sys}}{A_e}$

DIBAS-The Digital Backend System for Tianma

- Combination of GUPPI (pulsar system) and Vegas (spectra line system) of NRAO
- In comparison with GUPPI, DIBAS is an **updated system**. Maximum bandwidth that GUPPI can support is 800MHz (both coherent & incoherent de-dispersion).

Coherent:
- Both the inter- and intra-channel dispersion effects can be eliminated.
- Dense computation
- Accomplished with 8 GPU computers
- Maximum bandwidth supported : 800MHz

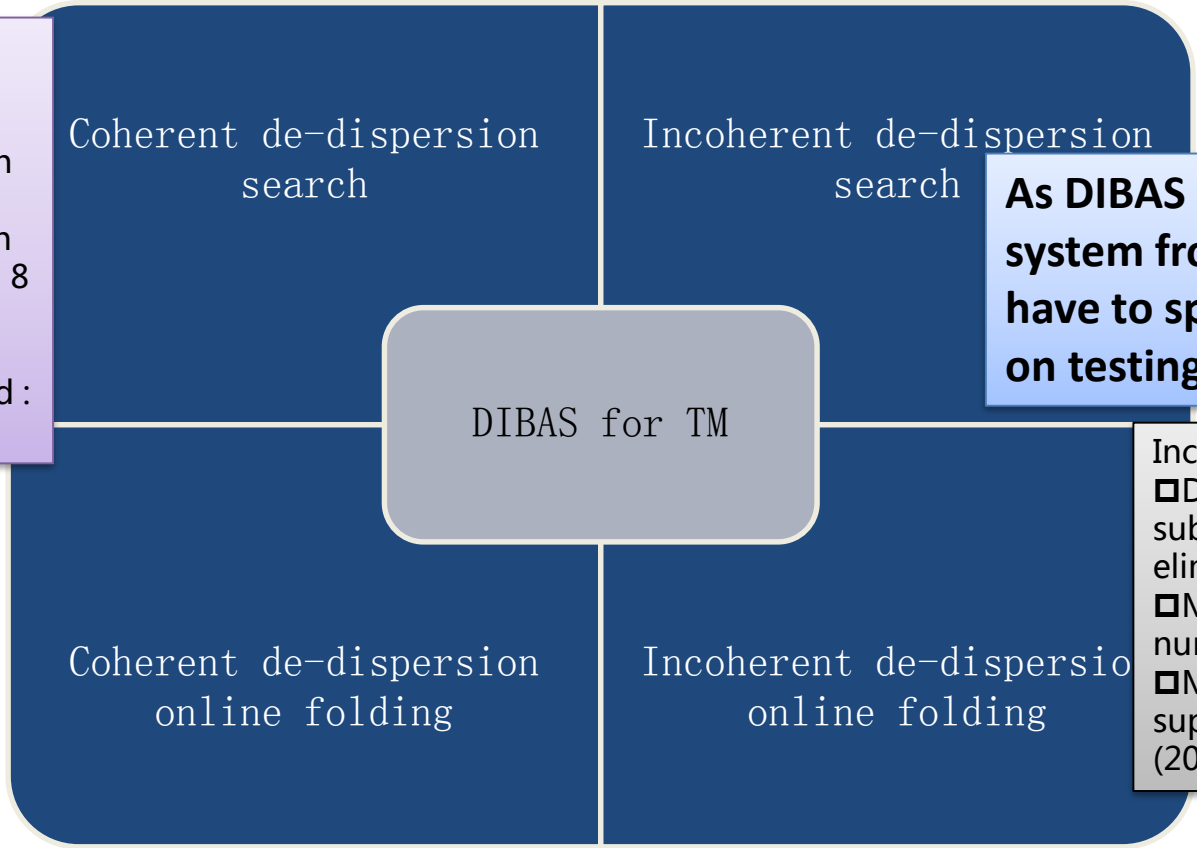

As DIBAS is an updated system from NRAO, we have to spent a lot of time on testing!

Incoherent:
- Dispersion effect in sub-band can not be eliminated;
- Maximum sub-channel number: 8192
- Maximum bandwidth supported : 6000MHz (2000MHz/Roach)

(GTX-580 GPU)

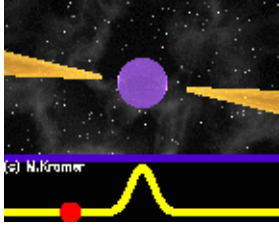

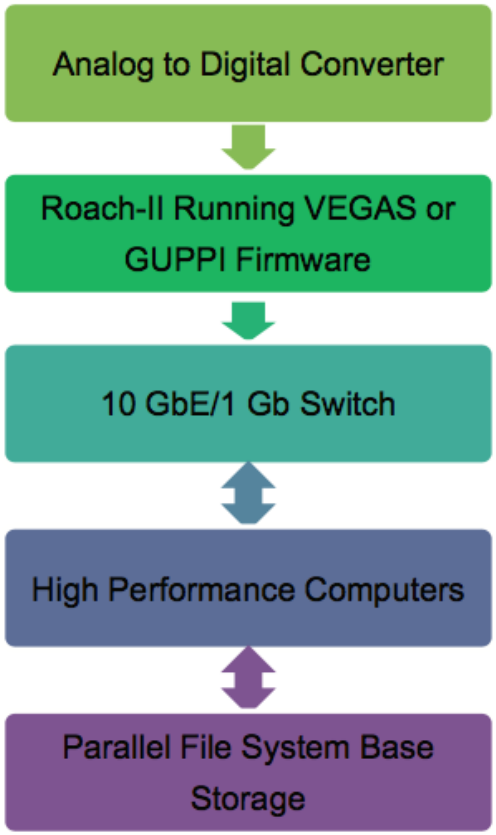

Figure 1. The block diagram of the DIBAS

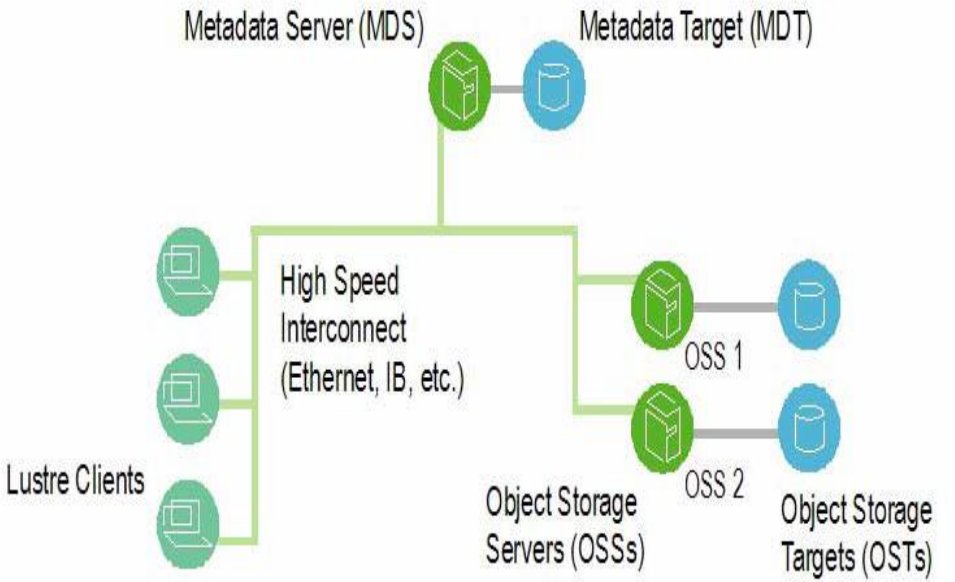

Fig.Lustre File System

- Maximum data recording speed: 300MB/s (per thread)
- Highest time resolution: 40.96μs

PSR B1937+21 profile got with Incoherent & Coherent observation mode

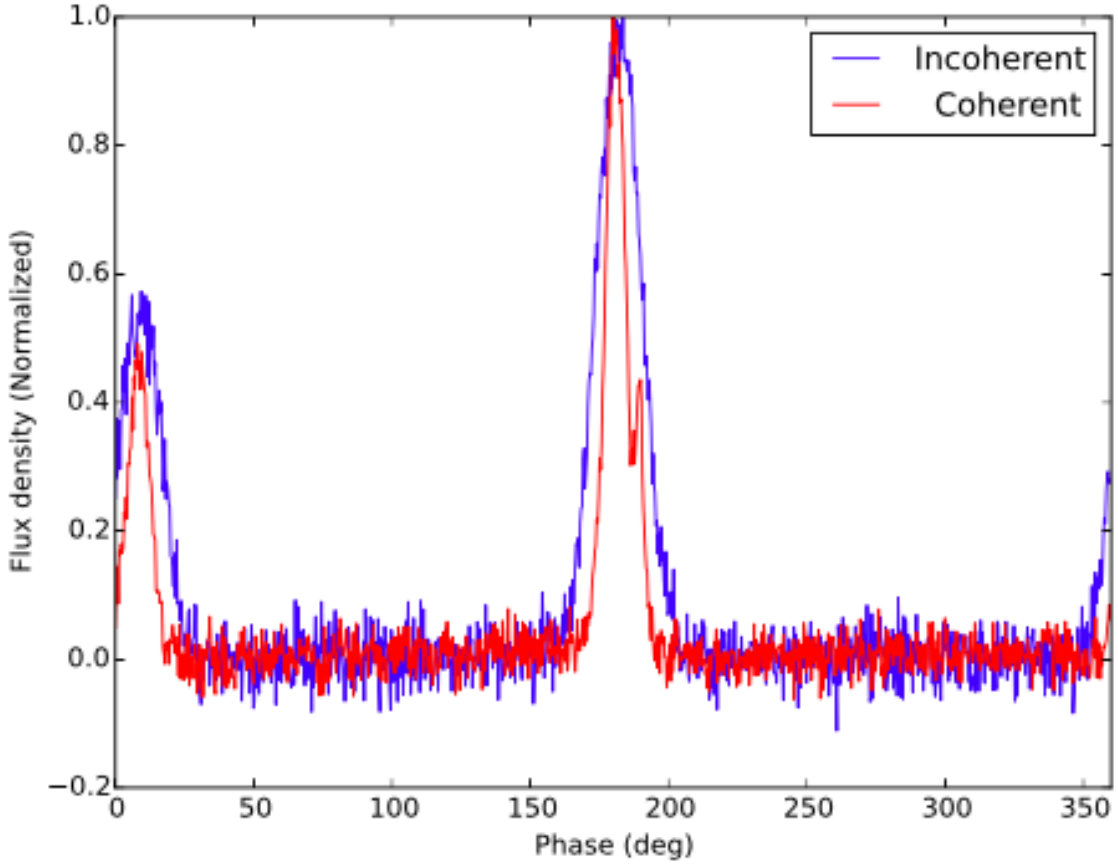

- The shortest rotational period pulsar on the northern sky: PSR B1937+21 (1.56 ms)
- S1400~13mJy, L-band observation, BW:~500MHz
- T-integration: 10 min

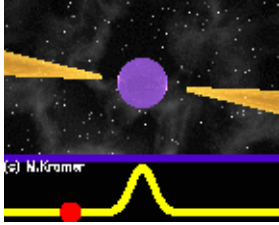

Magnetar J1745-2900 observation with TMRT

Magnetar J1745-2900 observation with TMRT

- A magnetar is a kind of neutron star with extremely strong magnetic field.
- The magnetic field decay powers the emission of high-energy radiation, particularly X-rays and gamma rays.
- Of the 28 magnetars and candidates previously known, only three of them have detectable radio pulsations (Olausen & Kaspi 2014).
- PSR J1745-2900 was firstly detected as an X-ray flare thought to be from Sgr A* by Swift . Follow-up observations with the NuSTAR X-ray Observatory detected periodic intensity variations with a period of 3.76 s (Kennea et al. 2013, Mori et al. 2013, Kaspi et al. 2014).
- The radio pulsations from J1745-*2900 were* detected by several large radio telescopes, which makes it the fourth magnetar known with radio pulsations (e.g., Eatough et al. 2013a).

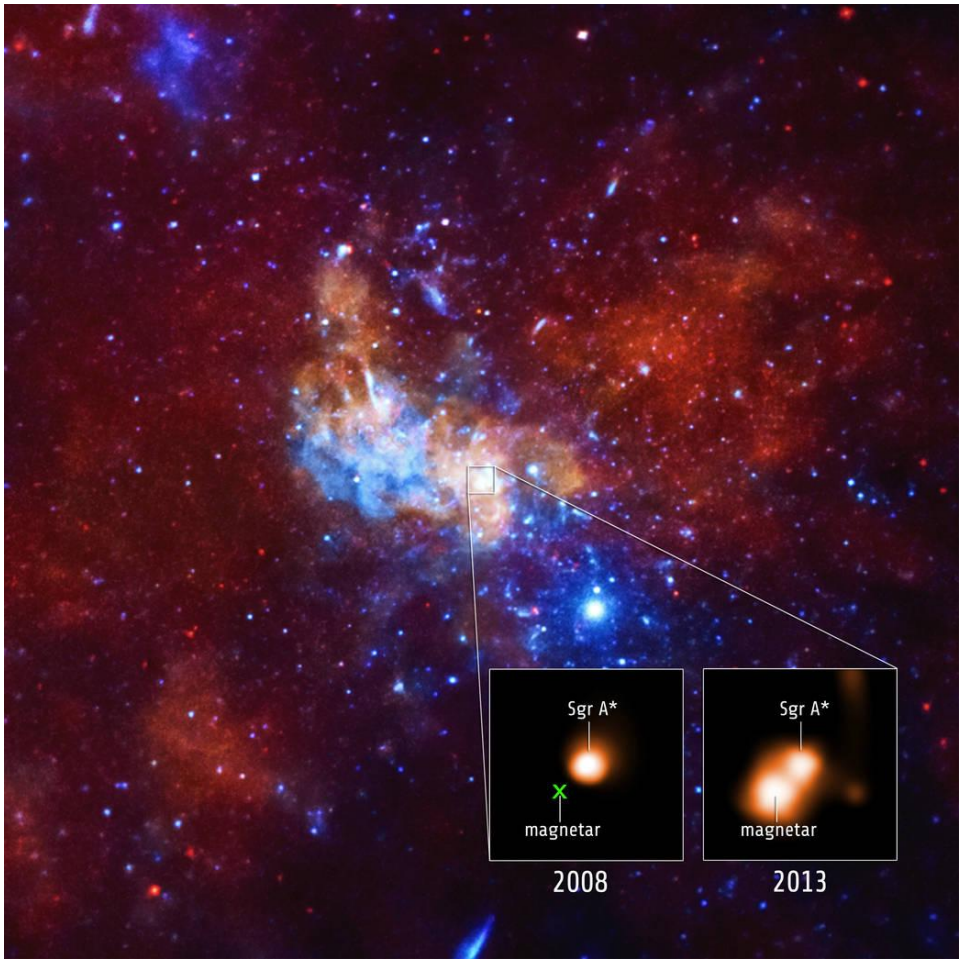

http://www.nasa.gov/mission_pages/chandra/magnetar-near-supermassive-black-hole-delivers-surprises.html

Observations and data reduction

- Observations were carried out using the new-built Shanghai Tian Ma Radio Telescope (TMRT) at a frequency of 8.6 GHz.
- DIBAS backend, Bandwidth: 8.2-9.0 GHz , divided into 512 channels .
- Pulsar search mode was used, with a time resolution 131.07 microseconds.
- Six epochs: MJDs of 56836, 56862, 56873, 56911, 56912 and 56943.
- Observation length 120, 40, 25, 26, 60 and 90 min, respectively.

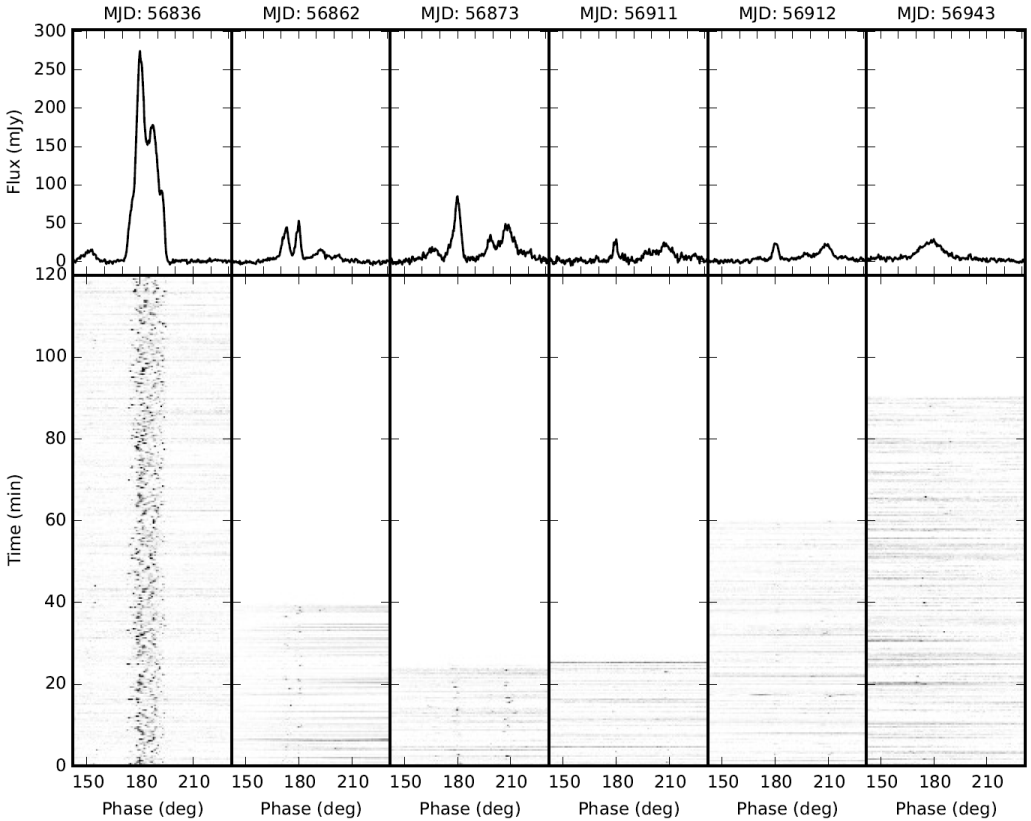

Such spiky emission is not common in phase-time plots of other pulsars.

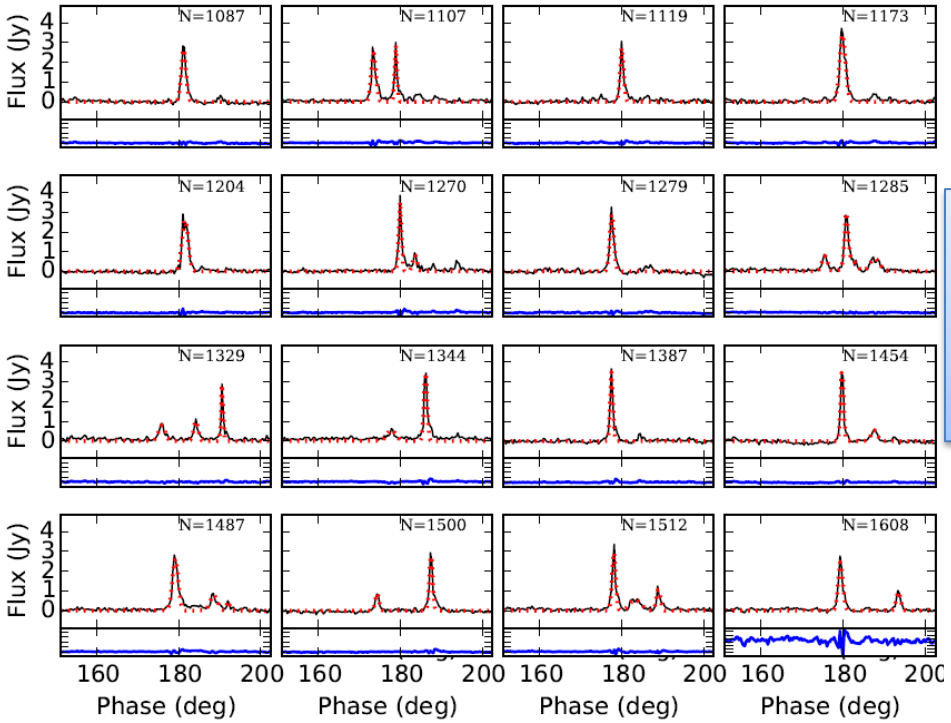

W50 of pulses whose peak flux density exceeds ten times that of integrated profile are in the range of 0.2 *to 0.9 deg. For comparison,* W50 for the integrated profile is about 12 *deg.*

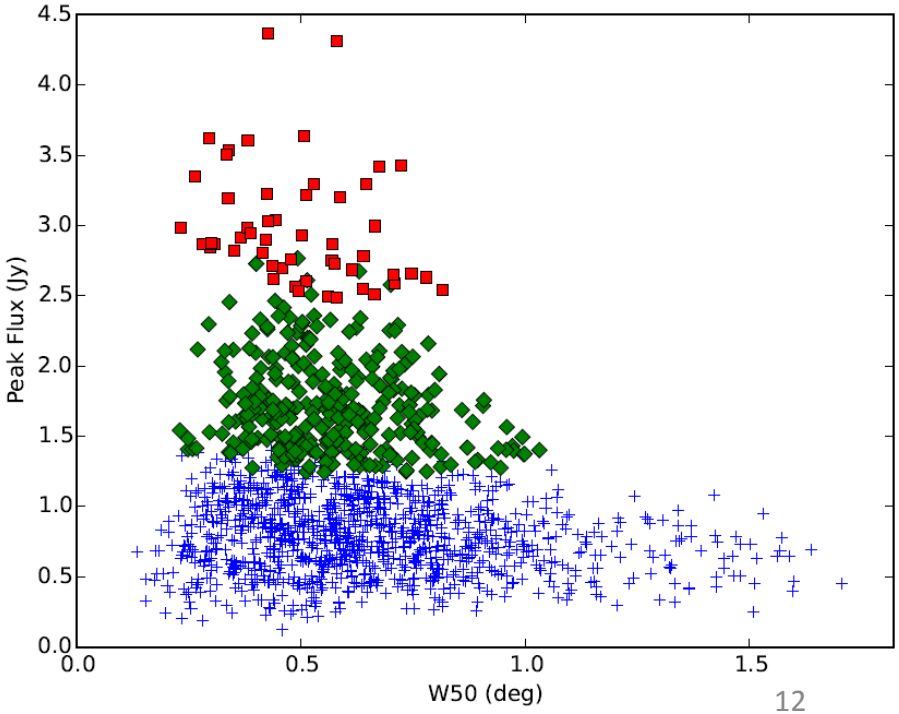

The W50 of pulses with lower peak flux density are in a comparable but somewhat wider range. *However, there is no clear* correlation between peak flux density and pulse width. Even though the peak flux density of these pulses is high, their pulse energy is not that large, as their pulse widths are much narrower than that of the integrated profile.

Histogram of central pulse phase for the 53 pulses with peak flux density greater than ten times the peak flux density of the integrated pulse profile.

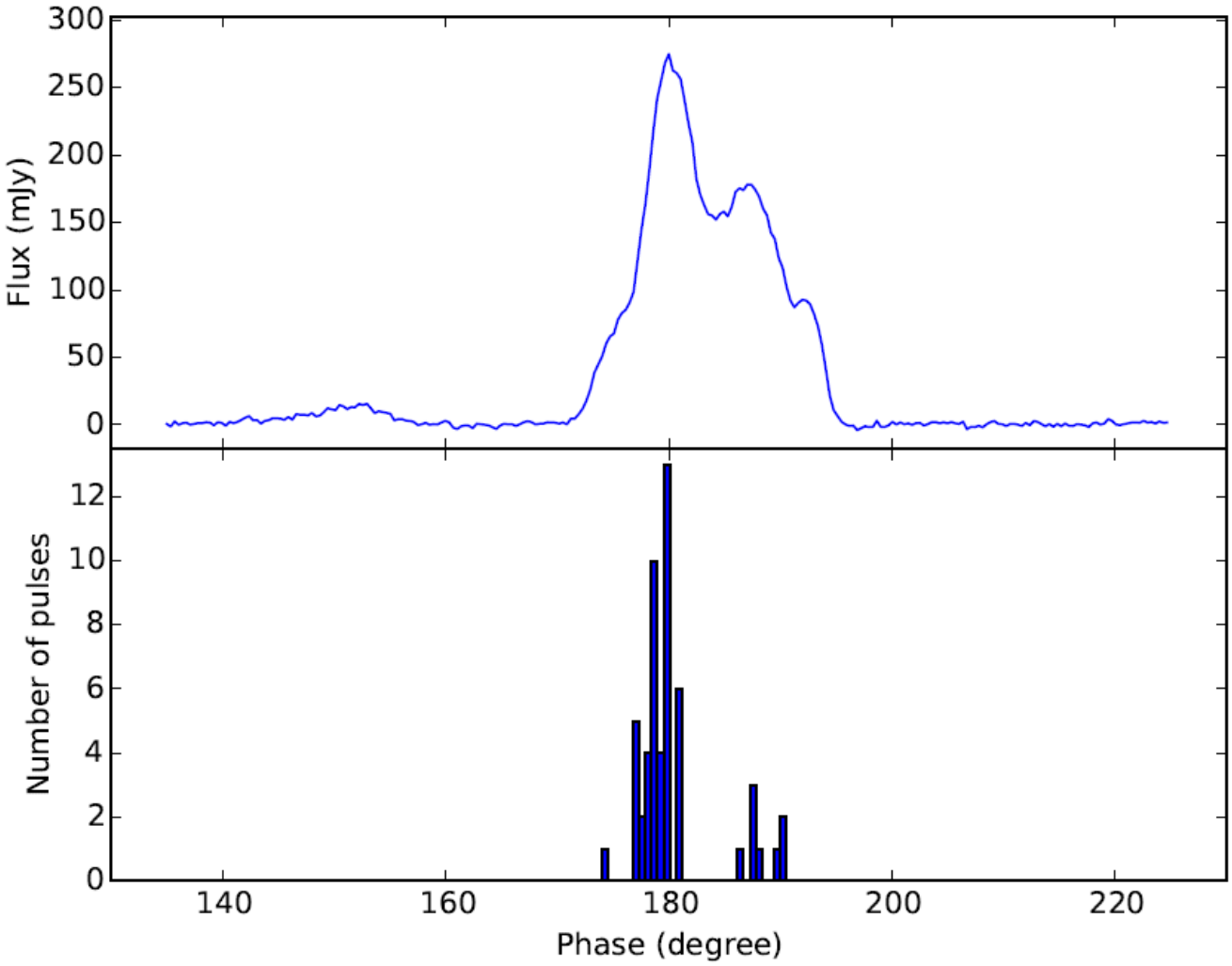

This shows that the strong pulses are preferentially emitted at the phases of the peaks in the integrated profile.

Sub-pulse drifting properties

- Sub-pulse drifting can be characterized by two numbers: the horizontal separation between adjacent sub-pulses in pulse longitude (*P2) and the vertical separation* between drift bands in pulse periods (*P3).*
- Useful diagnostics of sub-pulse modulation are longitude-resolved standard deviation (LRSD) and the longitude-resolved modulation index (LRMI). Useful diagnostic plots from the Fourier methods are the two-dimensional fluctuation spectrum (2DFS) and the longitude-resolved fluctuation spectrum (LRFS) which can be used to characterize *P2* and *P3, respectively (Weltevrede et*

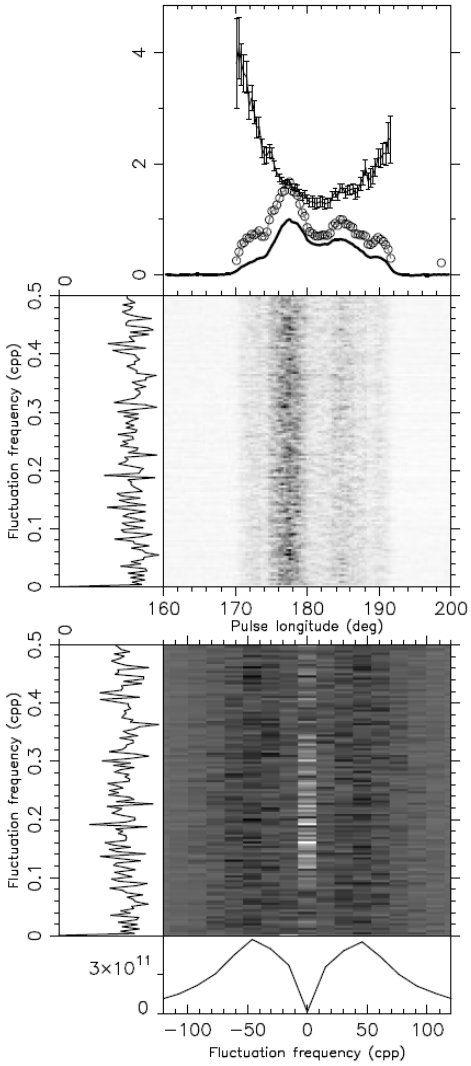

Zhen Yan et al. *2015, ApJ, 814*

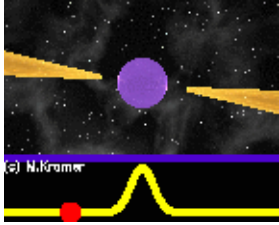

Multi-frequency pulsar observations

Multi-frequency observation of integrated pulsar profile and its radiation mechanism

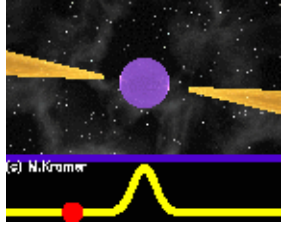

- **26 integrated pulse Profiles**
  - The quality of 26 profiles are comparable with the previous from Effelsberg or Parkes.
  - Mean flux densities of these pulsars are estimated and the calibrated pulse profiles are provided.
  - 11 profiles of this sample are obtained for the first time at 8.6 GHz.
- **Relationship between the component separation of 19 integrated pulse profiles and frequency**
  - firstly, the separation in 9 pulsar profiles decrease with the increasing of frequency, which is roughly agreement with radius-to-frequency mapping (RFM);
  - secondly, the separation in 10 pulsar profiles are nearly constant, which seems not in accordance with RFM, and could be due to the presence of the smallest separation.

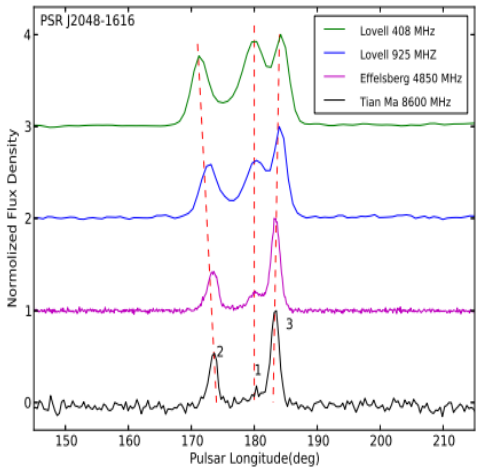

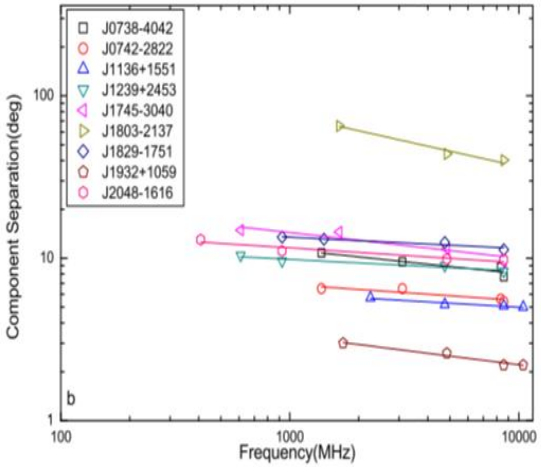

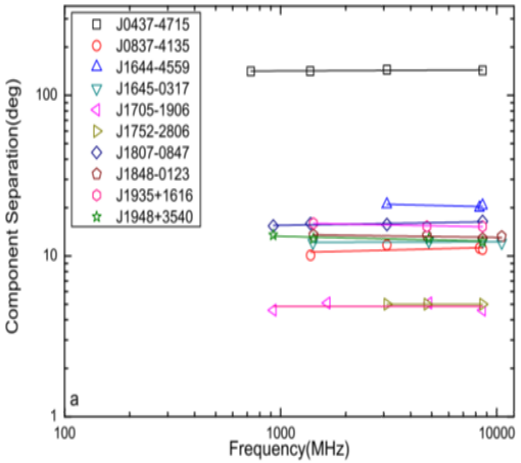

See Rushuang Zhao's talk for more information

Mode change of PSR B0329+54

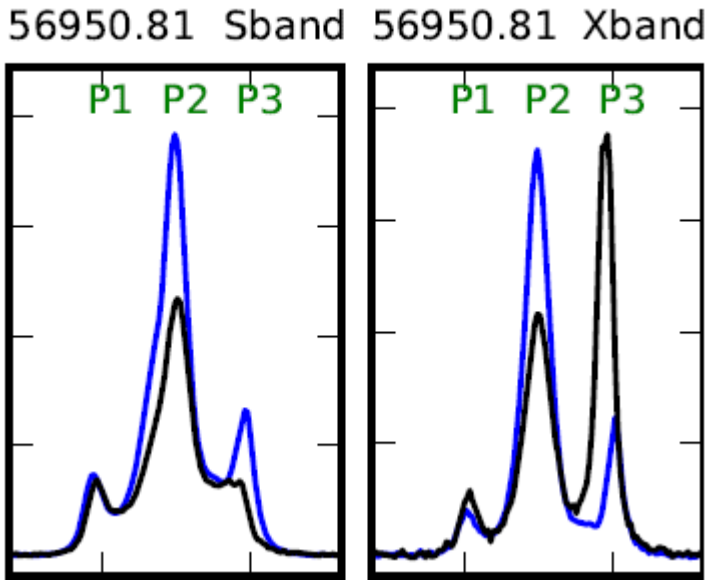

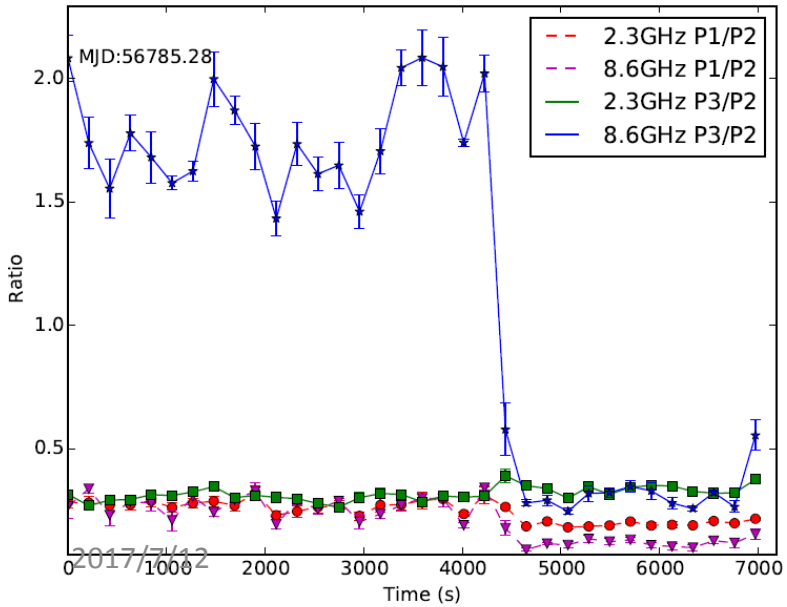

Num	MJD	$T_{\rm O}$ (s)	$t_{\rm samp}$ (μs)	$W_{\rm A}$	$T_{\rm A}$ (s)	$F_{\rm A/N,S}$	$F_{\rm A/N,X}$
1	56755.33	1636	65.536	Y	590	0.87 ± 0.01	1.26 ± 0.05
2	56759.10	4648	65.536	Y	875	2.33 ± 0.01	1.60 ± 0.04
3	56759.17	3729	65.536	N	0	-	-
4	56759.23	2857	65.536	N	0	-	-
5	56759.42	2641	65.536	Y	2641	0.76 ± 0.02	1.61 ± 0.03
6	56782.12	1866	32.768	N	0	-	-
7	56782.19	2556	32.768	N	0	-	-
8	56782.28	3399	32.768	N	0	-	-
9	56784.07	7187	65.536	N	0	-	-
10	56784.15	7187	131.072	N	0	-	-
11	56784.24	7187	131.072	Y	782	0.32 ± 0.01	1.75 ± 0.02
12	56784.32	4233	131.072	Y	875	1.43 ± 0.01	1.18 ± 0.02
13	56785.08	7188	131.072	Y	222	0.33 ± 0.01	0.92 ± 0.03
14	56785.12	7188	131.072	Y	1477	1.57 ± 0.01	1.03 ± 0.04
15	56785.20	7188	131.072	Y	4850	0.67 ± 0.01	0.96 ± 0.03
16	56785.28	7188	131.072	Y	4579	1.57 ± 0.01	1.04 ± 0.03
17	56786.04	7188	131.072	N	0	-	-
18	56786.12	1626	131.072	N	0	-	-
19	56786.31	5594	131.072	Y	444	1.00 ± 0.01	1.58 ± 0.02
20	56836.04	7188	131.072	N	0	-	-
21	56836.16	6733	131.072	Y	245	1.70 ± 0.01	1.03 ± 0.03
22	56850.11	3580	131.072	N	0	-	-
23	56863.06	2437	131.072	N	0	-	-
24	56863.10	7188	131.072	N	0	-	-
25	56863.96	4061	131.072	Y	2153	2.67 ± 0.02	1.66 ± 0.02
26	56950.62	5395	65.536	Y	900	1.68 ± 0.01	1.64 ± 0.05
27	56950.68	5395	65.536	N	0	-	-
28	56950.74	5395	65.536	N	0	-	-
29	56950.81	6189	65.536	Y	1486	0.69 ± 0.01	1.15 ± 0.03
30	56951.68	2396	65.536	Y	90	0.89 ± 0.01	1.23 ± 0.05

Dual-frequency mode change studies at single-pulse level

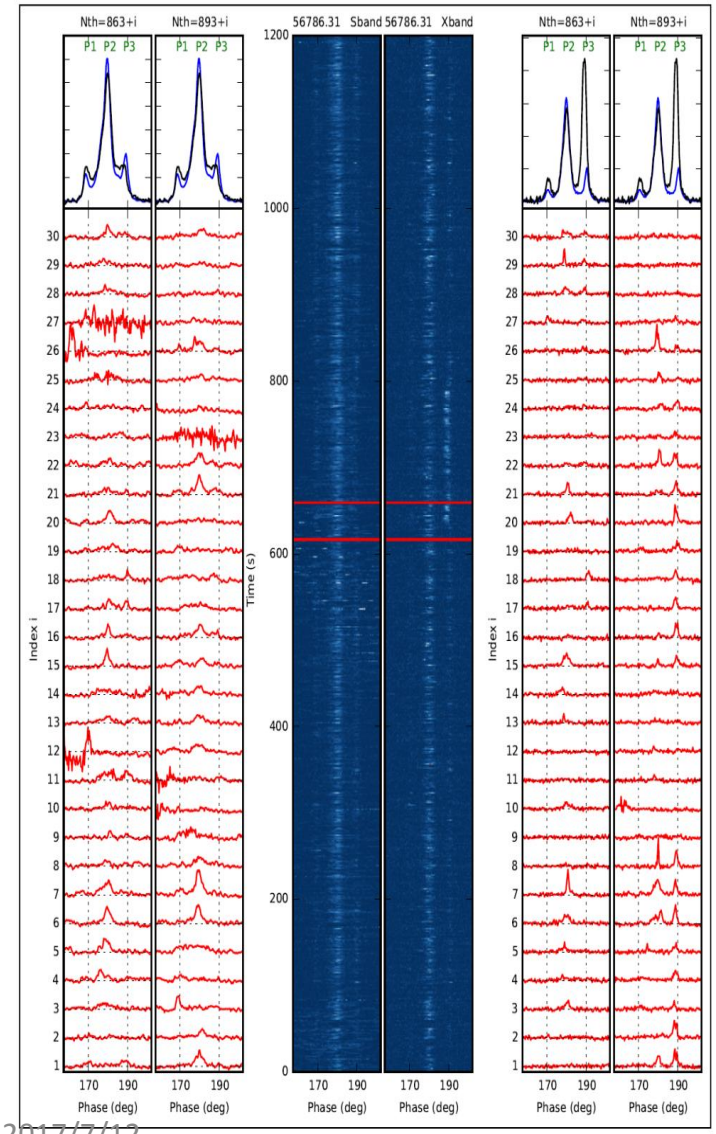

(a) Normal to abnormal mode

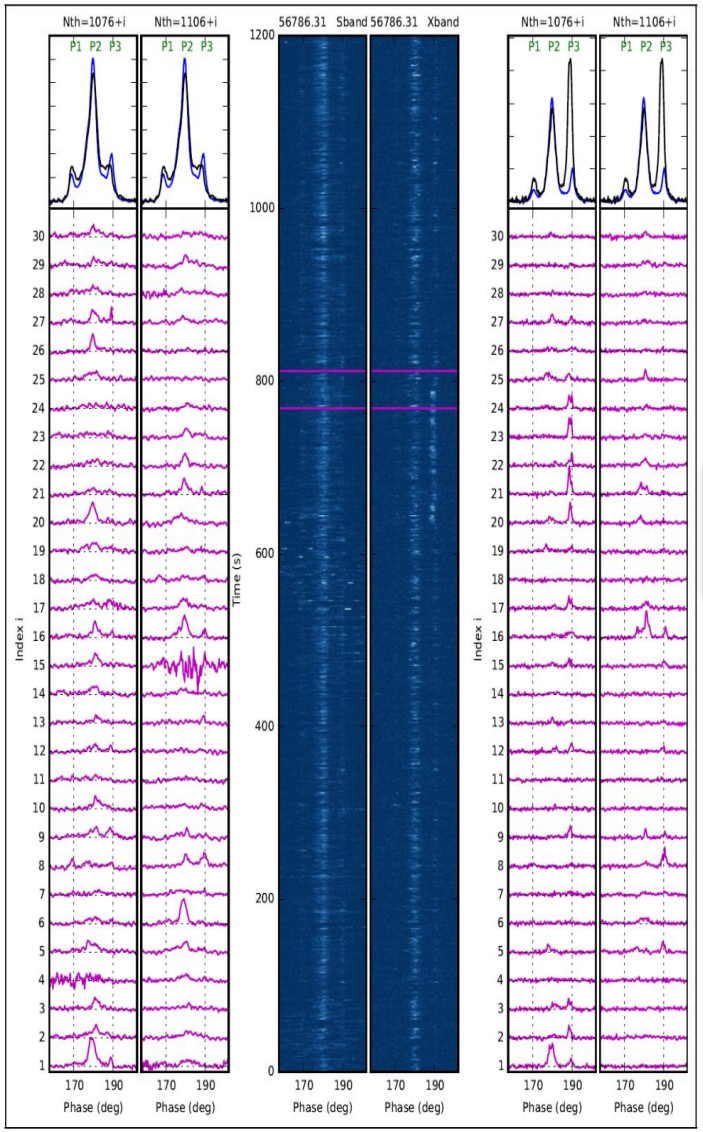

(b) Abnormal to normal mode

S/X-band

Regular Pulsar Timing

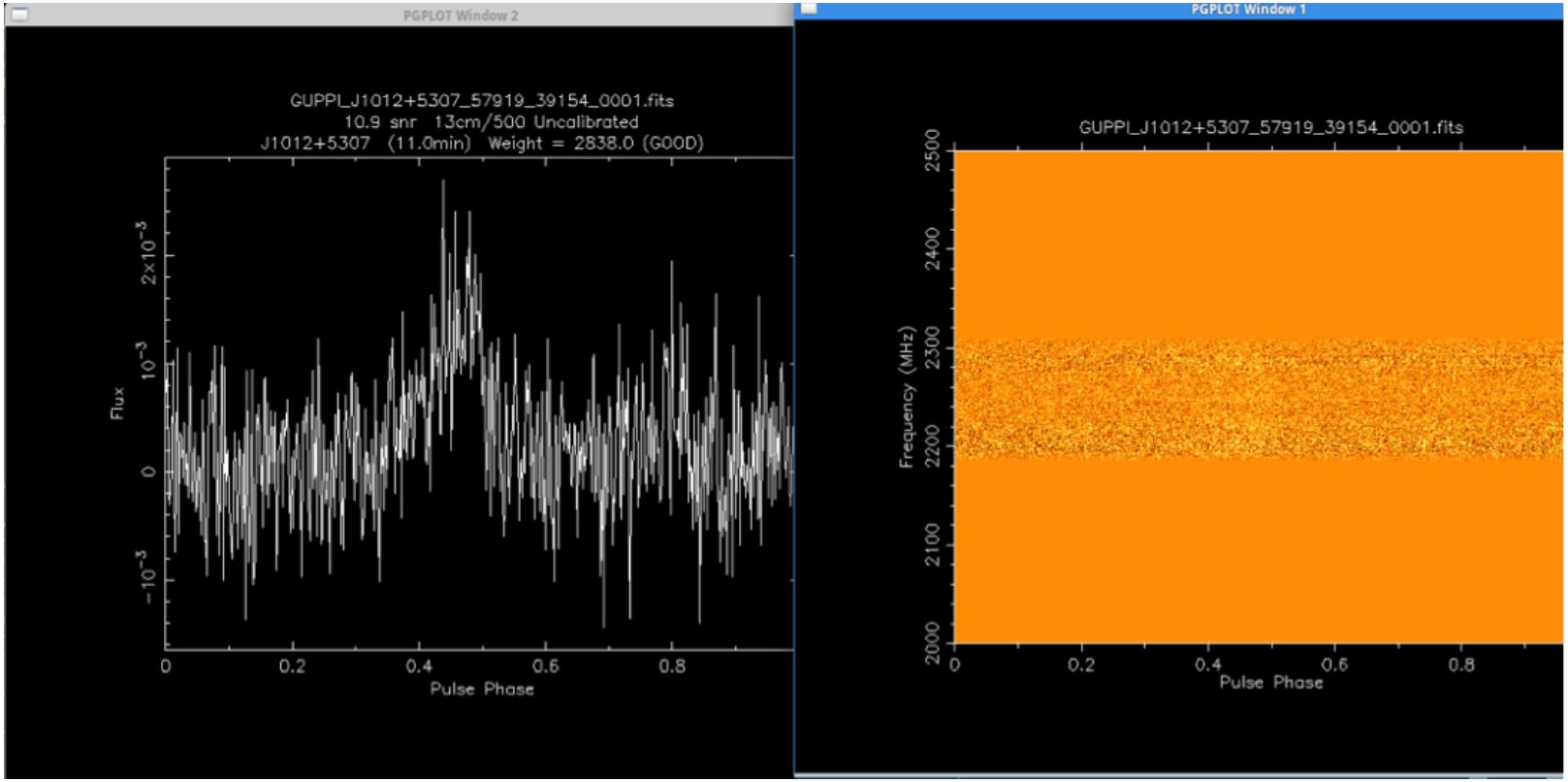

- MSP: J1012+5305, S2300=1.2mJy, Tint=11min, SNR>10;
- Normal Pulsar: B1530+27, S1400=0.8mJy, Tint=10min, SNR>10;
- Sband/Lband observation: more than 300 pulsars can be expected!
- Cband observation: about 100 pulsars are monitoring now.

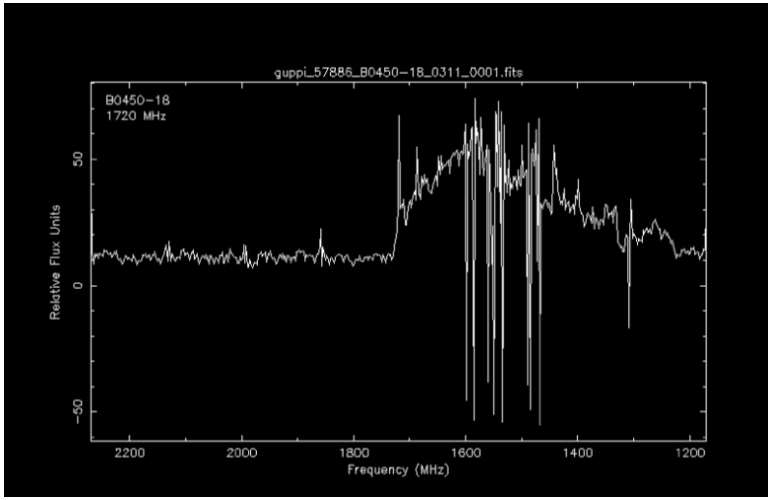

See Jie Liu's talk for more information

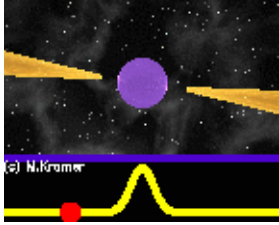

Pulsar Hunting

High Frequency Pulsar Hunting

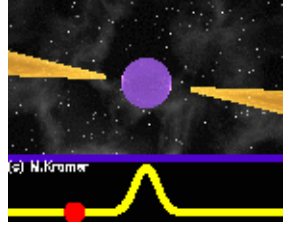

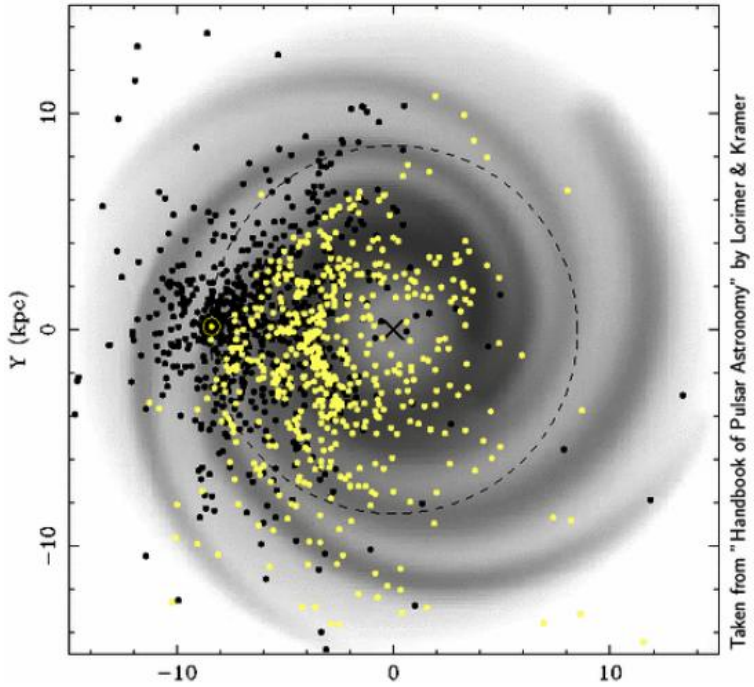

Yellow： discovered by 1.4GHz survey
Black： discovered by 430MHz survey

- Low frequency is blocked by thick plasma around the Galactic center
- lower galactic noise background, as the galactic noise is steeper power law
- weaker dispersion effect, as the dispersion delay is in proportion with the square of observation frequency
- weaker scattering, as the width of scattering broadening is in proportion of 4^{th} power of observation frequency;
- weaker scintillation

Unassociated γ-ray point sources

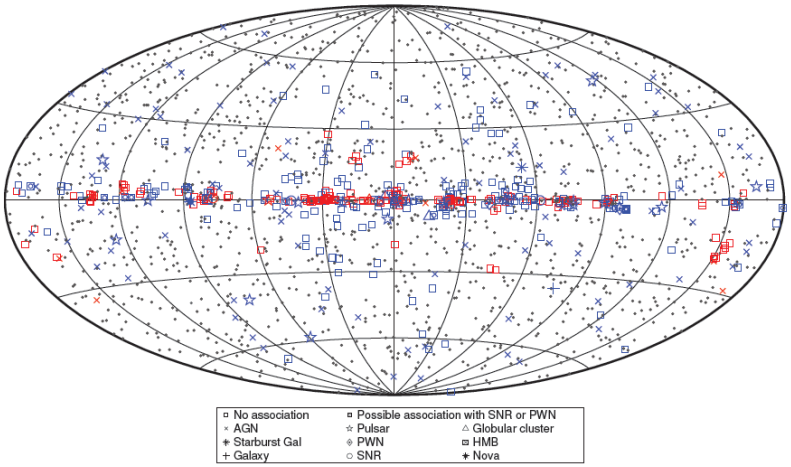

1873 sources, including 1062 associated with blazars and other AGNs, 11 GCs, 5 binaries, 576 «unassociated».

- GBT search 27 bright γ-ray unassociated source，3 new pulsar discovered（all of them are binary）!
- ~200 pulsars have been discovered in Globular clusters by now. Most of these pulsars are recycled pulsars (P<50ms)

Globular clusters

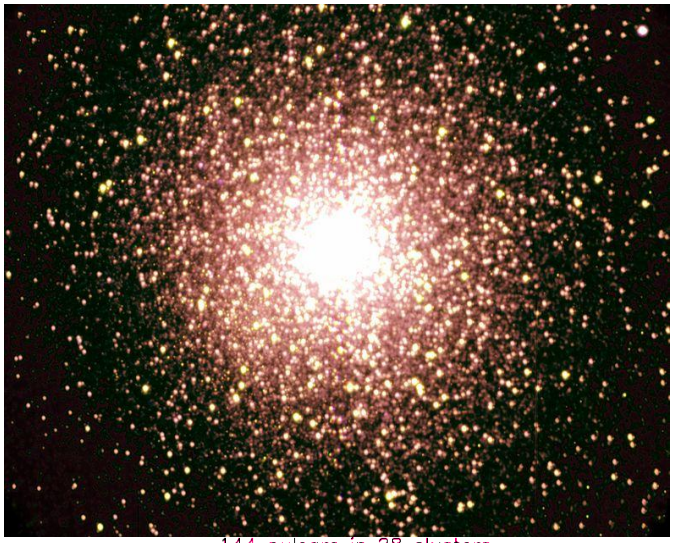

144 pulsars in 28 clusters

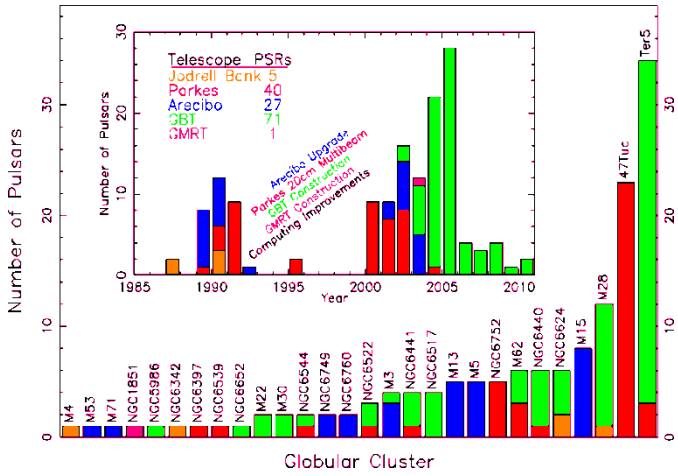

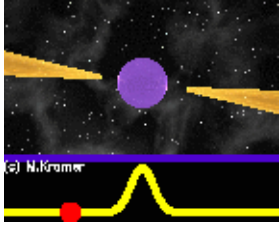

Pulsar Astrometry with VLBA plus TMRT

Challenges face for pulsar studies with VLBI

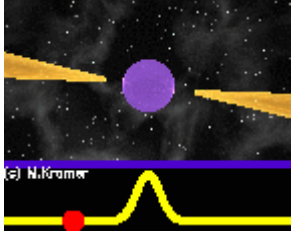

Faint, narrow pulse

- Average flux 0.8mJy (statistics on 908 pulsars)
- Duty cycle of most of pulsars less than 10%
- Pulsar gating in correlation (Booting SNR 3-6 times)
- Pulsar binning (More advanced gating)

Power-law spectra

- Power-law spectra(~-1.6), most observations at L-band
- Affected by ionosphere heavily
- Phase referenced (in-beam, nodding), GPS correction

Pulsar Astrometry with VLBA plus TMRT

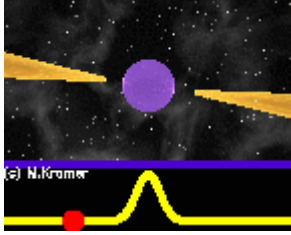

- For pulsars located at high declination (DEC>*45 deg), the resolution in right ascension (RA) will* be affected because of the limited length of projected baseline along East-West direction of VLBA .
- The partition of some Chinese antennas will lengthen the baseline twice times in East-West direction and make the UV-coverage of observation of source much better.
- Pathfinder observations on 2 high latitude pulsars are proposed by us.
- Highest data rate 2Gbps (previously 512 MHz) was used in our observation.
- Accuracy ~3 time higher than previous observation.

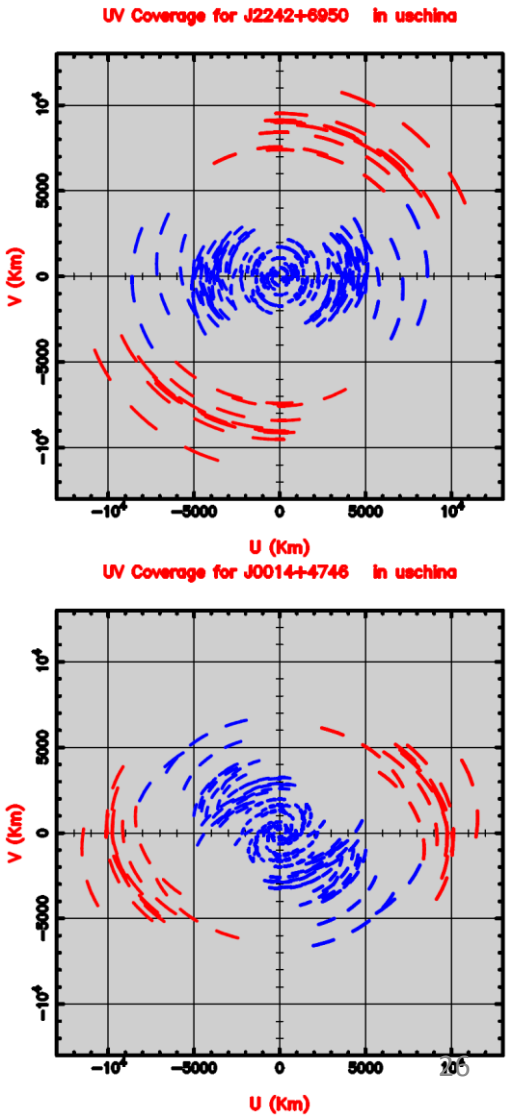

In cooperation with:
Zhi-Qiang Shen, Walter Brisken, Adam Deller, Miller Goss, Shami Chatterjee

Pathfinder observation results

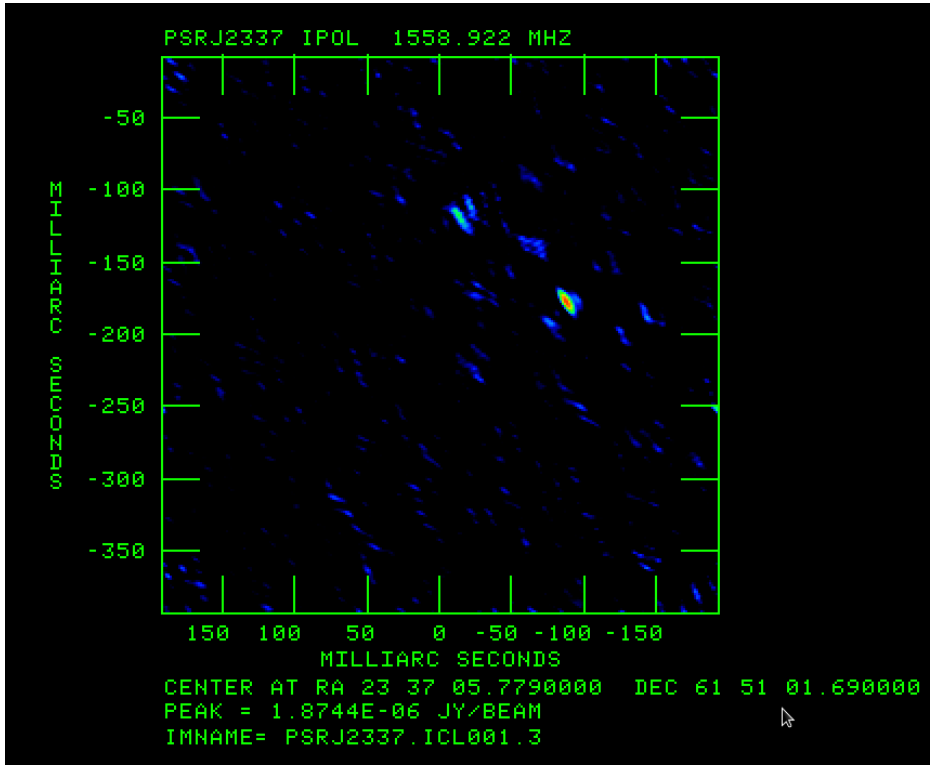

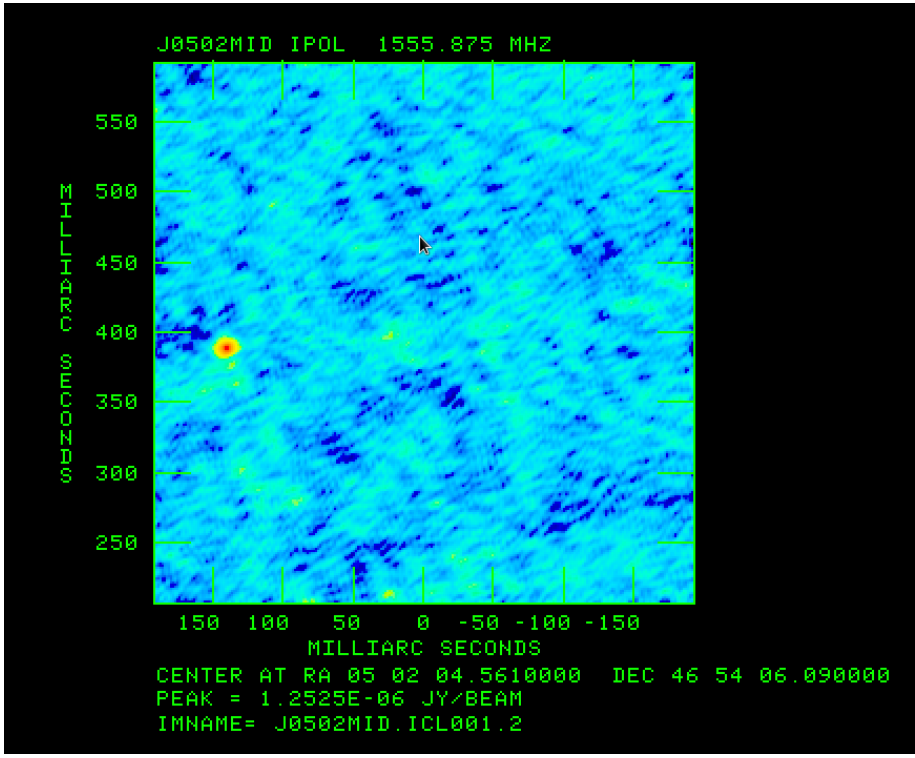

MULTI–FREQUENCY RADIO PROFILES OF PSR B1133+16: RADIATION LOCATION AND PARTICLE ENERGY

J. G. Lu[1,2], Y. J. Du[3], L. F. Hao[4], Z. Yan[5], Z. Y. Liu[6], K. J. Lee[7], G. J. Qiao[2], L. H. Shang[8], M. Wang[4], R. X. Xu[1,2,7], Y. L. Yue[9], and Q. J. Zhi[8]

Abstract

The pulse profile of PSR B1133+16 is usually regarded as a conal double structure. However, its multi-frequency profiles cannot simply be fitted with two Gaussian functions, and a third component is always needed to fit the bridge region (between two peaks). This would introduce additional, redundant parameters. In this paper, through a comparison of five fitting functions (Gaussian, von Mises, hyperbolic secant, square hyperbolic secant, and Lorentz), it is found that the square hyperbolic secant function can best reproduce the profile, yielding an improved fit. Moreover, a symmetric 2D radiation beam function, instead of a simple 1D Gaussian function, is used to fit the profile. Each profile with either well-resolved or not-so-well-resolved peaks could be fitted adequately using this beam function, and the bridge emission between the two peaks does not need to be a new component. Adopting inclination and impact angles based on polarization measurements, the opening angle ($\theta_{\mu 0}$) of the radiation beam in a certain frequency band is derived from beam-function fitting. The corresponding radiation altitudes are then calculated. Based on multi-frequency profiles, we also computed the Lorentz factors of the particles and their dispersion at those locations in both the curvature-radiation and inverse-Compton-scattering models. We found that the Lorentz factors of the particles decrease rapidly as the radiation altitude increases. Besides, the radiation prefers to be generated in an annular region rather than the core region, and this needs further validation.

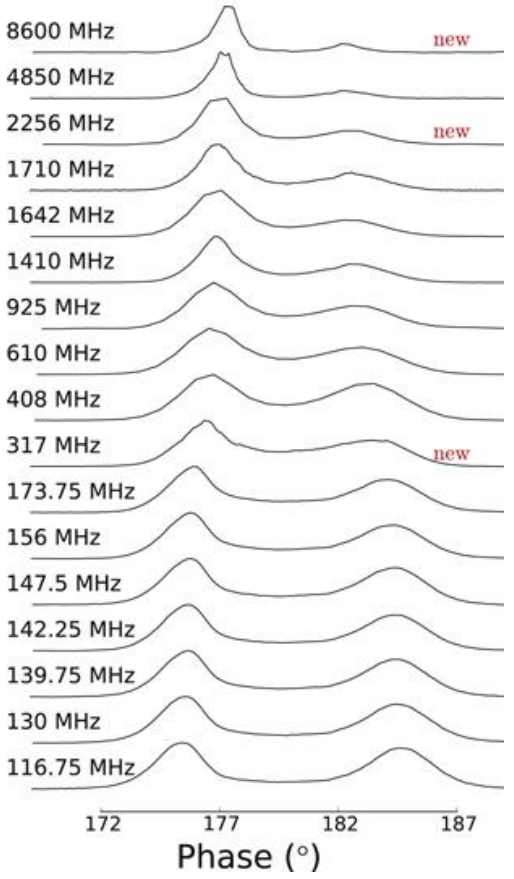

Title: Investigating the multifrequency pulse profiles of PSRs B0329+54 and B1642–03 in an inverse Compton scattering model

Authors: Shang, Lun-Hua; Lu, Ji-Guang; Du, Yuan-Jie; Hao, Long-Fei; Li, Di; Lee, Ke-Jia; Li, Bin; Li, Li-Xin; Qiao, Guo-Jun; Shen, Zhi-Qiang; Wang, De-Hua; Wang, Min; Wu, Xin-Ji; Wu, Ya-Jun; Xu, Ren-Xin; Yue, You-Ling; Yan, Zhen; Zhi, Qi-Jun; Zhao, Rong-Bing; Zhao, Ru-Shuang

Publication: Monthly Notices of the Royal Astronomical Society, vol. 468, issue 4, pp. 4389-4398 (MNRAS Homepage)

Publication Date: 07/2017

Origin: CROSSREF

DOI: 10.1093/mnras/stx815

Bibliographic Code: 2017MNRAS.468.4389S

Abstract

The emission geometries, e.g. the emission region height, the beam shape, and radius-to-frequency mapping, are important predictions of pulsar radiation model. The multi-band radio observations carry such valuable information. In this paper, we study two bright pulsars, (PSRs B0329+54 and B1642-03) and observe them in high frequency (2.5 GHz, 5 GHz, and 8 GHz). The newly acquired data together with historical archive provide an atlas of multi-frequency profiles spanning from 100 MHz to 10 GHz. We study the frequency evolution of pulse profiles and the radiation regions with the these data. We firstly fit the pulse profiles with Gaussian functions to determine the phase of each component, and then calculate the radiation altitudes of different emission components and the radiation regions. We find that the inverse Compton scattering (ICS) model can reproduce the radiation geometry of these two pulsars. But for PSR B0329+54 the radiation can be generated in either annular gap (AG) or core gap (CG), while the radiation of PSR B1642-03 can only be generated in the CG. This difference is caused by the inclination angle and the impact angle of these two pulsars. The relation of beaming angle (the angle between the radiation direction and the magnetic axis) and the radiation altitudes versus frequency is also presented by modelling the beam-frequency evolution in the ICS model. The multi-band pulse profiles of these two pulsars can be described well by the ICS model combined with the CG and AG.

Conclusions

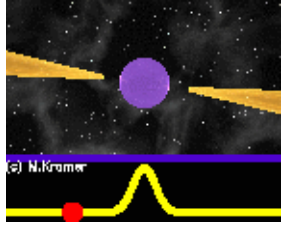

- Pulsar will be one of important scientific targets of TMRT
- Some pulsar observations with TMRT have been done. And good results have been obtained.
- TMRT can play an important role in the fields of pulsar research, such as pulsar searching, giant pulse, RRAT, pulsar timing, astrometry plus VLBA et al.
- Looking forward your cooperation!

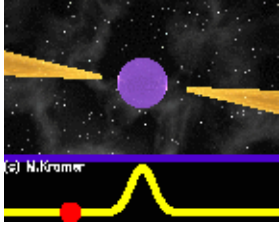

THANK YOU!